DOI: ADD DOINUMBER HERE

Nitromethane as a Green Propellant: First Results of a Combustion Test Campaign

Maxim Kurilov†, Lukas Werling* and Christoph Kirchberger*†*
* DLR Institute of Space Propulsion
74239 Hardhause a.K., Germany
maxim.kurilov@dlr.de, lukas.werling@dlr.de, christoph.kirchberger@dlr.de
† Corresponding Author

Abstract

Because of hydrazine's carcinogenic and toxic nature its use in space propulsion is expensive and may lead to significant delays. One already established alternative is to use energetic salt-based ionic liquid propellants, dissolving ammonium dinitramide or hydroxyl ammonium nitrate in water with additives. However, with this approach costs remain high because these substances are quite costly and highly regulated due to their partly unstable and energetic nature. Nitromethane, being a widely available solvent, offers a cost-effective solution, with comparable propulsive performance. In this paper results of a hot-fire test campaign are presented. Stable combustion using NMP-001 a nitromethane-based monopropellant at 15 – 40 bar pressure at 84 – 94 % C*-efficiency in a combustion chamber with L* = 9 to 11.7 m was demonstrated.

1. Introduction

In the satellite industry, there has been a significant increase in the adoption of "green" propulsion systems and propellants over the past two decades. This shift can be attributed to the toxic and carcinogenic nature of hydrazine [1], which has prompted concerns regarding its handling and regulatory requirements. The drawbacks associated with hydrazine have made it less attractive in the modern and fast-paced satellite industry, especially driven by the "NewSpace" sector. Conversely, the use of non-toxic "green" propellants not only has the potential to reduce project costs [2], particularly in satellite constellations [3], but also offers a significant improvement in terms of health risks for propellant handlers.

Table 1: Physical properties of nitromethane [4]

Formula	CH_3NO_2
Melting point	-28.3 °C
Boiling point	101.2 °C
Density	1137 kg/m^3

Two primary research directions are being pursued to develop monopropellant alternatives for hydrazine. These directions focus on using energetic materials dissolved in water and mixed with organic fuel components and additives. In one approach, primarily undertaken in Europe, researchers are exploring the use of ammonium dinitramide (ADN), an energetic salt, along with liquid fuel components like methanol or ammonia. The water in which ADN is dissolved also acts as a phlegmatizing agent. A study conducted by [5] thoroughly analyzed, characterized, and optimized the formulation and properties of the ADN-based FLP propellant family. Later, the Swedish company ECAPS developed

and used the LMP-103S propellant in satellites [6, 7]. In another approach, prominently pursued by JAXA [8] and NASA [2], hydroxyl ammonium nitrate (HAN) is employed as the energetic component. Notably, the Japanese SHP propellant family and the American propellant AF-M315 (ASCENT) have reached a high technology readiness level. For example, ASCENT was already demonstrated in orbit as part of the GPIM mission [9] and is being developed for use in powering bi-modal chemo-electrical propulsion systems in CubeSats [10]. SHP-163, on the other hand, was used on a balloon-dropped aerodynamic test bed in 2010 [8] and later demonstrated in space on the RAPIS satellite [11]. In both cases, a pre-heated precious-metal-based catalyst pack is employed to initiate the thrusters.

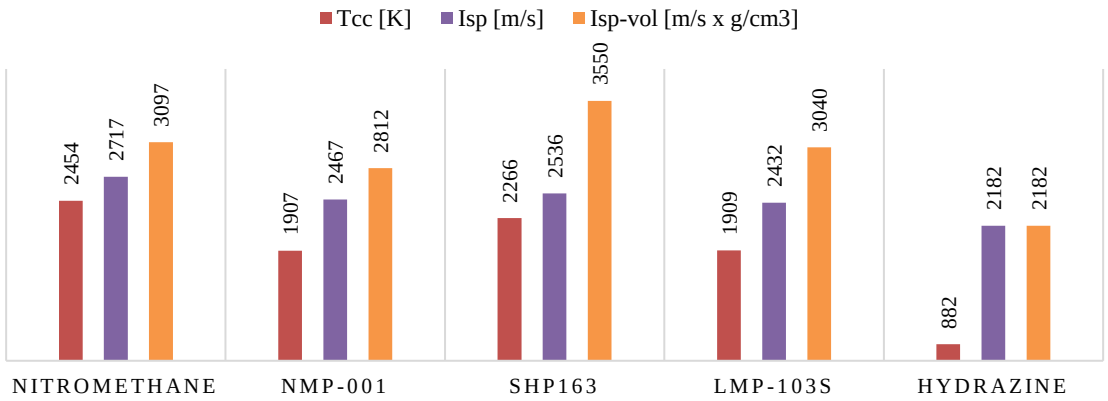

Figure 1: Propellant performance parameters, 20 bar, 200:1, equilibrium flow, calculated with NASA CEA [19]

Since the 1930s, nitromethane has been considered a promising monopropellant [12]. In the 1940s and 1950s, research programs in the U.S. focused on designing and developing nitromethane-powered rocket chambers, gas generators, and torpedo systems [13, 14]. Further investigation took place in Israel in the late 1950s. In [15] and [16] violent decomposition reactions in the cooling jacket of regeneratively cooled combustion chambers are described. These incidents were attributed to the quite large $V_{cc}/A_{throat} = L^*$ requirement to fully combust nitromethane-based propellant mixtures (4 to 26 m; 6 m for pure nitromethane). Before the rise of interest in "green" orbital propulsion in the 1990s and 2000s, the primary research emphasis within the orbital propulsion community revolved around hydrazine, which is the main reason nitromethane was neglected as a rocket propellant in the 1960s and 70s. However, in the 1980s, the potential of nitromethane as a viable alternative to hydrazine was recognized, and preliminary investigations to assess catalyst bed materials were initiated [17, 18]. Subsequently, in the 2000s an extensive analysis of nitromethane's combustion characteristics in a strand-burner device at pressures between 2 and 120 MPa was conducted; additionally, nitromethane thoroughly was evaluated, which confirmed its high potential for propulsion applications [12].

In summary, nitromethane is a good potential "green" propellant due to its lower toxicity compared to hydrazine. It is more readily available compared to ADN and HAN because it is a staple laboratory solvent. Additionally, its wide liquid range eases thermal requirements on propellant systems (see Table 1). Figure 1 presents the mass- and density-specific impulse and combustion chamber temperature of nitromethane, hydrazine, LMP-103S, and SHP-163. The calculations were carried out using the NASA CEA tool [19]. As shown, the performance of pure nitromethane is comparable to the two ionic propellants, making it promising for satellite and spacecraft applications. The performance of NMP-001, a nitromethane-based propellant containing additives, which was used in the campaign presented in this paper, is also listed. Although this propellant was not optimized for performance being just a first iteration in designing an orbital propellant, it surpasses hydrazine in both mass- and volume-specific impulse. In fact, the theoretical performance figures are similar to LMP-103S.

Early nitromethane research encountered several challenges, including the difficulty of finding a reliable and straightforward ignition method and achieving stable combustion at pressures below 30 bar [14, 20, 21]. This difficulty can be attributed to the strong pressure dependence of nitromethane decomposition, which crucially is governed by intermolecular collisions [22, 23]. Notably, in a strand burner, the burning rate of nitromethane significantly increases with higher pressures [12]. To address these challenges, proposed solutions in [20, 21] involve the use of dissolvable transition-metal salts and other catalysts to enhance decomposition. Pilot-flame based ignition methods were employed as an ignition source in this research. The first method utilizes a chemical flamethrower-based initiator, while the second method uses a pilot nitromethane-oxygen flame to initiate combustion in the main chamber. In subsequent investigations conducted by [17, 18] at the laboratory scale, a catalytic approach to nitromethane exothermal decomposition was explored. Although nitromethane could be successfully decomposed over Ni- and Cr-based materials, these catalysts were quickly deactivated by carbon depositions. Consequently, our research group chose to

employ a pilot flame for initiation and, similar to the aforementioned sources, dissolve a catalytic substance to facilitate nitromethane decomposition. In [24], a screening and characterization of suitable substances are presented. The most significant findings revealed that the addition of 2 wt.% ferrocene, iron-(III)-acetylacetonate, or vanadyl-(III)-acetylacetonate caused the decomposition peak in closed-crucible DSC measurements to shift by 100, 65, and 61 °C, respectively, compared to pure nitromethane.

Another challenge arises from the fact that nitromethane is an energetic substance, which means it can deflagrate or detonate when subjected to mechanical stimuli or heating [25, 26]. To address this challenge, an approach suggested by [12, 14, and 25] is to add inert substances to nitromethane. In [27], we conducted a detailed exploration of this approach and identified the required levels of admixture for so-called inhibitors, such as n-butanol, dimethyl sulfoxide, and nitroethane, to enable safe bench test experiments. It was found that as little as 5 wt.% n-butanol, 6 wt.% dimethyl sulfoxide, and 35 wt.% nitroethane were needed to decrease the BAM-Fallhammer impact sensitiveness of nitromethane from ≤ 1J to > 10 J. The performance penalty incurred was only 3 – 8 % in terms of specific impulse decrease, depending on the specific additive used.

This paper presents the results of a combustion chamber test campaign conducted with NMP-001. This propellant primarily consists of nitromethane but also includes an inhibitor and an ignition catalyst. NMP-001 is classified as "green" according to the definition provided in [28] since it does not contain substances that are harmful upon contact with skin, nor does it contain any components proven to cause cancer, genetic effects, or fertility damage. Nonetheless, personal protective equipment such as nitrile gloves, goggles and a standard respirator needs to be employed.

Due due to added substances, the performance of NMP-001 is reduced compared to pure nitromethane. On the other hand, the BAM-Fallhammer impact sensitivity of NMP-001 is above 10 J, which is far superior than in pure nitromethane. The objective of this campaign was to assess the performance and combustion stability of NMP-001 at pressures typical for satellites and spacecraft, specifically combustion chamber pressures ranging from 10 to 40 bar. The combustion chamber used in this study had a similar specific length as those used in the 1940s and 1950s studies [16, 21], with $V_{CC}/A_{throat} = L^*$ ranging from 9 to 11.5 m. In satellites and spacecraft, a pressure-fed propulsion system is preferred due to its simplicity, necessitating lower combustion chamber pressures of 10-20 bar. As a general guideline, a pressure difference by a factor of 1.5 between the combustion chamber and the propellant tank is required to ensure safe operation [29, 30]. However, as mentioned earlier, nitromethane can only support stable combustion at pressures exceeding 30 bar. Operating at such high pressures would require a propellant tank pressure of around 45 bar, resulting in a significant overall system mass penalty due to the need for a thick-walled tank. Therefore, special attention was given to determining the low-pressure combustion limit of NMP-001.

2. Experimental setup

The test campaign described in this paper was conducted at the M11.4 test bench located at the DLR test complex in Lampoldshausen. This test facility is equipped with a redundant Siemens PLC for control purposes. The facility is multifunctional and includes high-pressure gas sources capable of reaching pressures up to 200 bar, supplying gases such as H_2, O_2, N_2, and Air. Additionally, if needed, the facility can provide cooling water at pressures up to 60 bar. To ensure comprehensive data acquisition, a NI-PXI-based DAQ system is employed, allowing for the utilization of up to 160 sensor channels.

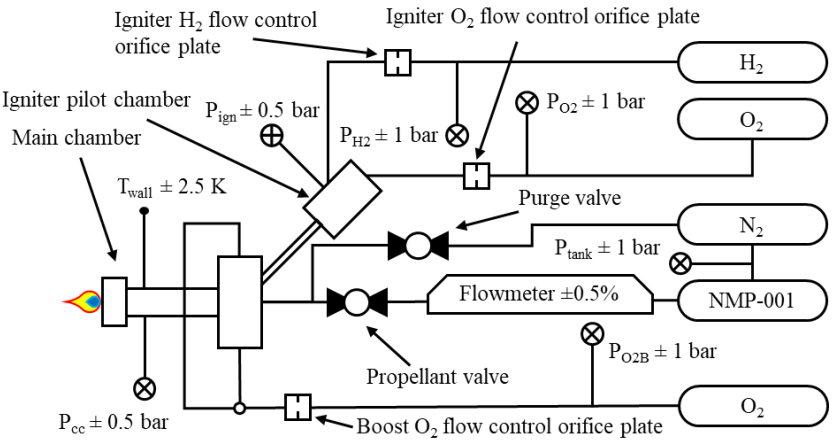

Figure 2: Test setup overview

In the current test setup, we utilized up to 10 STS-TM pressure sensors with an accuracy of ≤ 0.5% of the full measurement range (refer to figure 2, not all sensors are shown). The signals from these sensors are amplified using DEWETRON amplifiers before being processed by the data acquisition system (DAQ). For measuring the crucial quantities, such as the combustion chamber pressure (Pcc) and the ignitor pilot chamber pressure (P_{ign}), we employed 100 bar sensors, resulting in an uncertainty of ±0.5 bar for these measurements. In all other cases, 200 bar sensors were utilized, introducing an uncertainty of ±1 bar for the respective quantities. To measure the temperature of the combustion chamber wall, we employed 0.5 mm type K thermocouples with an accuracy of ±2.5 K. As shown in figure 3, these thermocouples were positioned inside the combustion chamber wall. They were placed within bores that extend into the wall, stopping 1.0±0.05 mm before reaching the inner surface of the chamber. In order to ensure uniform contact with the wall material, the thermocouples were loaded with a force of 2 N using springs (see figure 3), following a similar approach described in [31]. To facilitate integration with the DAQ system, the thermocouples were connected to thermoelement transmitters, which convert the signals into an output format readable by the data acquisition system.

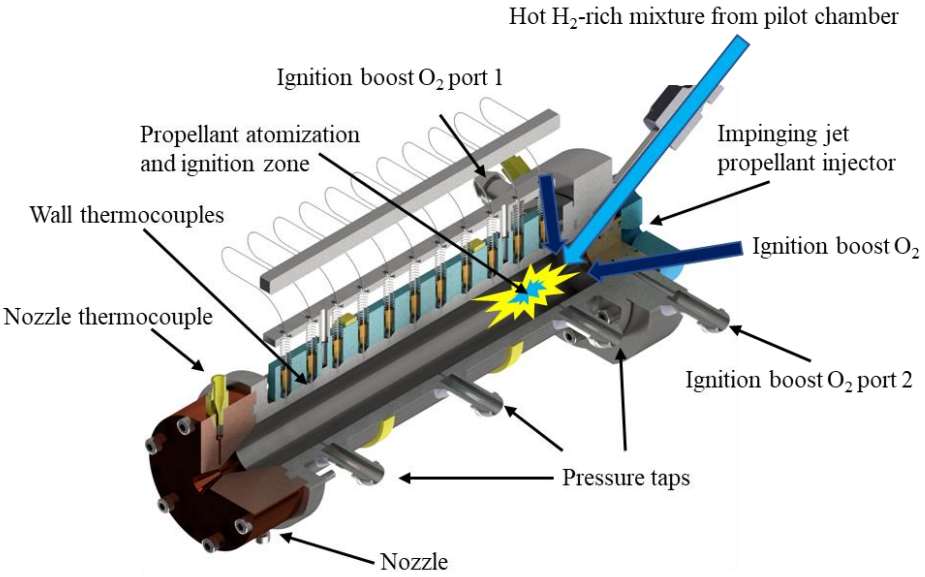

Figure 3: Detail view of the combustion chamber

The mass flow of propellant exiting the nitrogen pressurized NMP-001 tank is measured using a RHEONIK RHM03L Coriolis flowmeter. This flowmeter guarantees an accuracy of at least 0.5% of the currently measured value. The pressure inside the N2, H2, and O2 reservoirs is regulated by the Siemens PLC through controllable dome pressure reducers. To control the mass flow of oxygen and hydrogen gases, interchangeable orifice plates are employed. These metering orifices, are manufactured in-house with a precision of ±0.014 mm. They are designed for orifice diameters ranging from 0.5 to 1.0 mm. The discharge coefficients of these straight bore orifices were also determined in-house. These measurements, conducted at 16°C, yielded a discharge coefficient of 0.875±0.05. This value aligns well with the value of 0.85 presented in [32] for straight bores. Throughout the test campaign, the temperature inside the test cell varied between 12°C and 21°C. Consequently, the overall measurement uncertainty for gas mass flow amounts to ±11%.

The combustion chamber utilized in the conducted test is constructed from 1.4841 heat-resistant stainless steel. It measures 150 mm in length and has an inner diameter of 22 mm. The nozzle, on the other hand, is crafted from the CuCr1Zr high-temperature copper alloy. Despite the implementation of heat-resistant materials, the nozzle throat experienced significant erosion, resulting in variations in the inner diameter observed during the tests, ranging from 2.80 to 3.18 mm. To assess the inner throat diameter between each test, precision metering gauges with a diameter difference of 0.02 mm were employed. Thus, the measured value for the inner throat diameter has an uncertainty of ±0.02 mm. The range of nozzle diameters corresponds to a characteristic combustion chamber length, L^*, ranging from 9.0 to 11.7 m. For propellant injection, a single element impinging jet injector was utilized.

To initiate combustion, a two-stage H_2/O_2 gas torch igniter was employed. This ignition method bears similarities to the one utilized in [21], but with hydrogen replacing nitromethane to generate the pilot flame. The pilot chamber (see

figure 2) is operated hydrogen-rich (ROF ≈ 1). The mixture is ignited with the assistance of a spark plug and directed through a metal tube into the main combustion chamber (figure 3). Upon entering the main chamber, this hot mixture combines with additional oxygen from a separate pressure source, which is injected near the injector surface to enhance ignition (referred to as boost oxygen). The tests presented achieved a thermal performance of up to 125 kW during the ignition phase, with a ROF = 8.

3. Test sequences and analysis methodology

To assess performance at different pressures and determine the stable combustion limit at low pressures, the tank pressure was gradually reduced from one load point to another. Figure 4 presents the key temperature and pressure data for test 314_1, which was carried out at 40 bar tank pressure and serves as an illustrative example to explain the test sequence of the 31X test series. The test was initiated at zero ms by activating the spark plug, igniting the pilot chamber. To facilitate ignition, both the pilot chamber and the ignitor boost oxygen stage, where oxygen is directly injected into the main chamber, were operated with a slight oxygen lead. This means that the oxygen valves were actuated before zero. The hydrogen valve was actuated at 0 ms. At t_0 (118 ms in this specific test), the pressure in the main chamber significantly increased, defining t_0 as the ignition point. To preheat the combustion chamber, the igniter remained operational for a specific duration until NMP-001 injection was triggered at t_1. In the 31X test series, this interval had to be adjusted between 900 to 1200 ms to find an effective injection point. At t_2, the igniter pilot chamber was switched off, followed by the igniter boost stage at t_3. In the 31X test series, these actions were performed simultaneously. In this test series, the main propellant valve was closed at 4000 ms. After flameout at t_4, the injector and chamber were purged with nitrogen. Throughout all phases of the experiment, the combustion pressure was monitored by the control system. If an upper or lower pressure limit was reached, i.e. a redline crossed, the main valve was closed, the injector line was purged, and the propellant tank was depressurized, as was the case in test 618_1 shown below in figure 6.

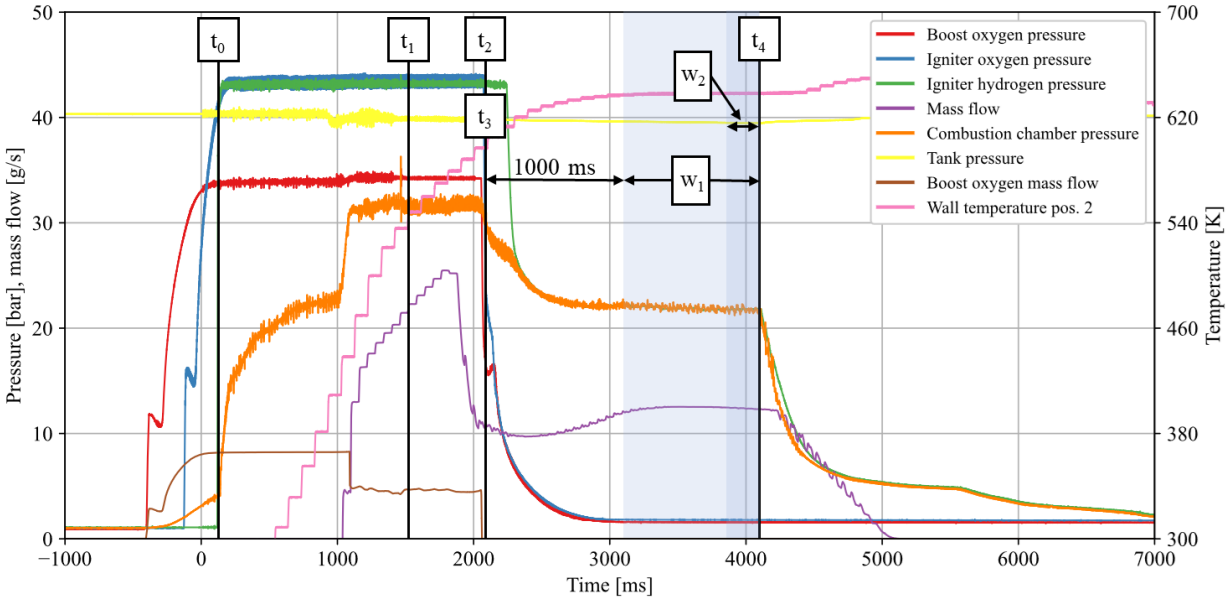

Figure 4: Test 314_1, ignition and test sequence and analysis logic 31X test series

In the 31X test series, when the tank pressure dropped below 25 bar, the combined operation of the ignitor boost stage and NMP-001 between t_1 and t_2 resulted in an almost negligible injector pressure drop. As a result, none or only a severely reduced quantity of the propellant was supplied to the combustion chamber at some point, which by itself could trigger severe instabilities. This occurred because the injector design only considered steady-state combustion chamber pressure as the driving parameter, neglecting the higher pressures during ignitor operation. Additionally, the design generally was intended for higher mass flows than those used in this test series, leaving no safety to assure a pressure drop under these circumstances. An approach to reduce the pressure-rise during the ignition sequence, was to gradually reduce the boost oxygen pressure. This first worked quite well, however, at some point this also led to severe limitations. A significant drop in oxygen mass flow immediately after the NMP-001 injection occurred with ever lower boost oxygen pressure. This is because this time the combustion chamber pressure reduced the pressure

difference between the oxygen pressure source and the combustion chamber until only subcritical flow or even no flow at all through the boost oxygen metering orifice occurred, which severely limited the gas throughput. Consequently, an insufficient amount of oxygen could be provided to support proper ignition. As a result, the threshold for low-pressure monopropellant operation could not be determined in the 31X test series.

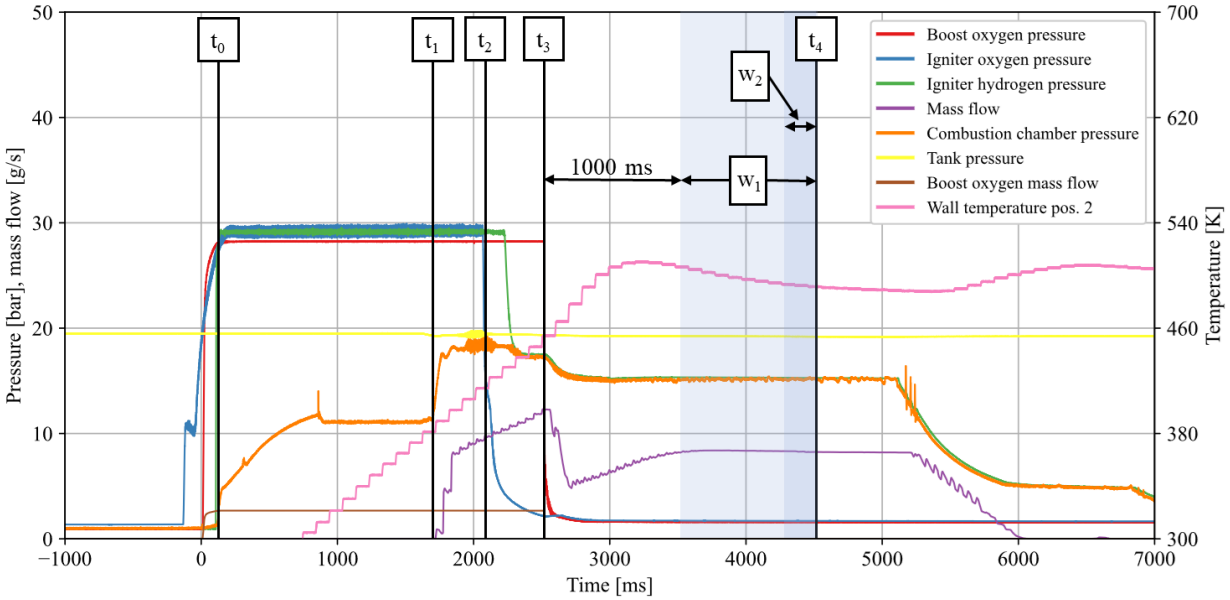

Figure 5: Test 620_2, ignition and test sequence and analysis logic 6XX test series

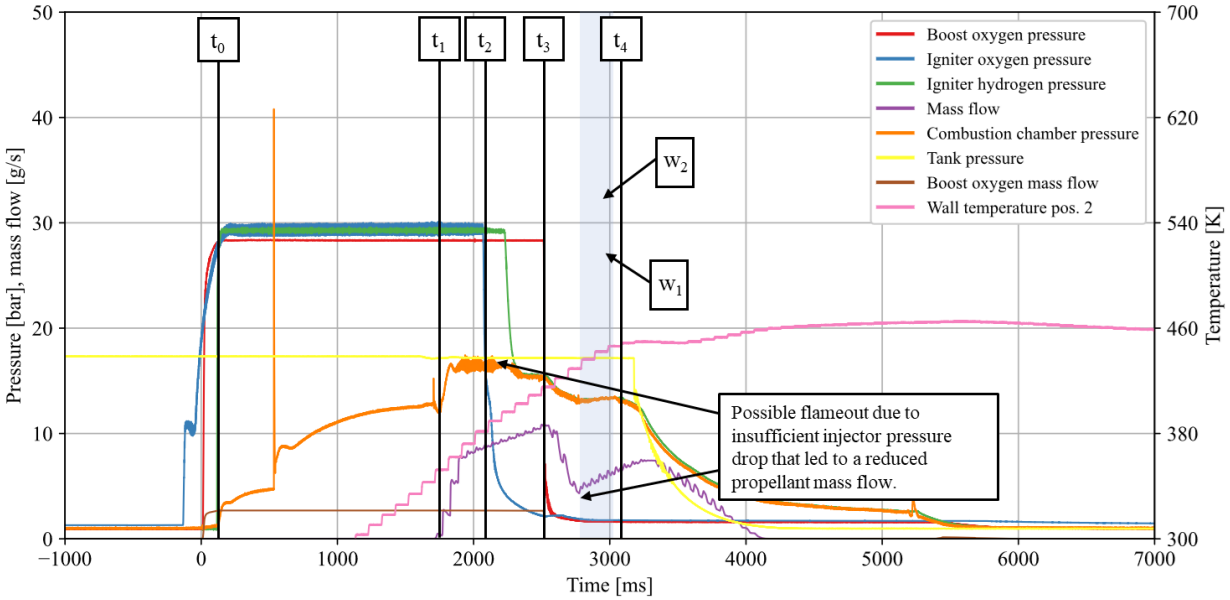

Figure 6: Test 618_1, no-go test analysis window

To investigate lower combustion chamber pressures than in the 31X series, a new test series called 6XX was conducted. In this series, a smaller boost oxygen metering orifice was employed to ensure that the pressure difference between the combustion chamber and the oxygen source remained sufficiently high. This enabled critical orifice flow, ensuring an adequate supply of oxygen for ignition between t_1 and t_3. The revised ignition sequence is illustrated in figure 5. In the 6XX test series, the propellant injection was delayed until 1700 ms, allowing the combustion chamber to reach a higher temperature between t_0 and t_1. The parallel operation time of the pilot chamber, boost oxygen, and propellant combustion was reduced: the pilot chamber was turned off at 2000 ms (t_2), followed by the boost oxygen at 2500 ms (t_3). Each regular experiment in this test series was concluded at 5000 ms

(t_4). The same ignition procedure was maintained throughout all the tests in this series. However, as demonstrated in figure 6, at some point as the tank pressure and propellant mass flow decreased, again the injector became unable to produce a significant pressure drop, thereby compromising a steady propellant mass flow.

To ensure a meaningful comparison between the two different test sequences in both test series, similar analysis windows were utilized. In all tests, the window w1 was positioned 1000 ms after the initiation of monopropellant operation (t_3). This quite long window, spanning 1000 ms, was employed for calculating and evaluating the chamber wall heating rate, pressure change rate, and oscillation intensity because these quantities require a longer time to show sensible effects. Furthermore, a 250 ms wide window, referred to as w_2, was placed in the last quarter of w_1. This window allowed for the assessment of combustion efficiency and oscillation intensity towards the end of each test run with a special emphasis on combustion effects towards the end of the experiment.

In certain test runs with non-stable combustion, the interval between t_3 and t_4 was less than 2000 ms. In such cases, both windows were shortened to 250 ms and precisely positioned right before the flameout (t_4), as depicted in figure 7.

Table 2: Combustion stability rating criteria

Criterion	**Score**
Monopropellant combustion time < 2000 ms	-2
Heating Rate (HR) < 0, inside window w1	-1
Oscillation intensity (OI) > 5%, inside window w2	-1
Pressure change < -5%, inside window w1	-1

Rating	**Outcome**
3/3	Stable combustion
2/3	Partly stable, non-self-sustaining combustion
1/3	Non-stable combustion

To evaluate the rocket performance the measured characteristic velocity C^* (equation 1) was compared to the theoretical value C^*_{CEA} calculated with the Gordon-McBride algorithm [19]. The comparison produces the combustion efficiency η_{C*}(equation 2). It is important to note that both the C^* and η_{C*} values are affected by uncertainties, as described earlier in relation to measurement accuracy.

$$C^* = \frac{P_{CC}}{\dot{m}} \times \pi \frac{d^2_{nozzle}}{4} \quad \textbf{(1)}$$

$$\eta_{C*} = \frac{C^*}{C^*_{CEA}} \times 100 \quad \textbf{(2)}$$

To determine the lower limit of operation under low pressure, it is essential to assess and rate the combustion stability. However, considering safety concerns and the early stage of development for NMP-001, the propellant injection time was restricted to 3.2 - 3.5 seconds. While this duration is sufficient for demonstrating burn times typically used in pulse operation mode, it does not adequately represent longer duration burns. Consequently, the test data must be thoroughly analysed to identify any instabilities that could cause a shutdown during longer burn times than those tested. To evaluate both short- and long-duration combustion stability, each test was initially assigned a

stability score of three points. An overview of the scoring system and rating criteria can be found in Table 2. If the combustion time of the monopropellant (from t_2/t_3 to t_4) is shorter than 2 seconds, it is considered non-stable, resulting in a subtraction of two points from the overall score. If this criterion is not met, the long-duration combustion stability is evaluated using three additional parameters.

The first parameter concerns the heating rate of the combustion chamber wall. Figure 7 illustrates the spatial temperature distribution along the axis of the combustion chamber, where 0 mm represents the injector face. The temperature data is derived from various test runs conducted in series 31X and 6XX. It's worth noting that certain temperature measurement channels were excluded from the analysis due to malfunctioning. Despite the absence of some data, the observed temperature distribution indicates that a significant portion of the energy release occurs between the 20 and 60 mm positions along the chamber axis, which corresponds to temperature sensors 1 – 5.

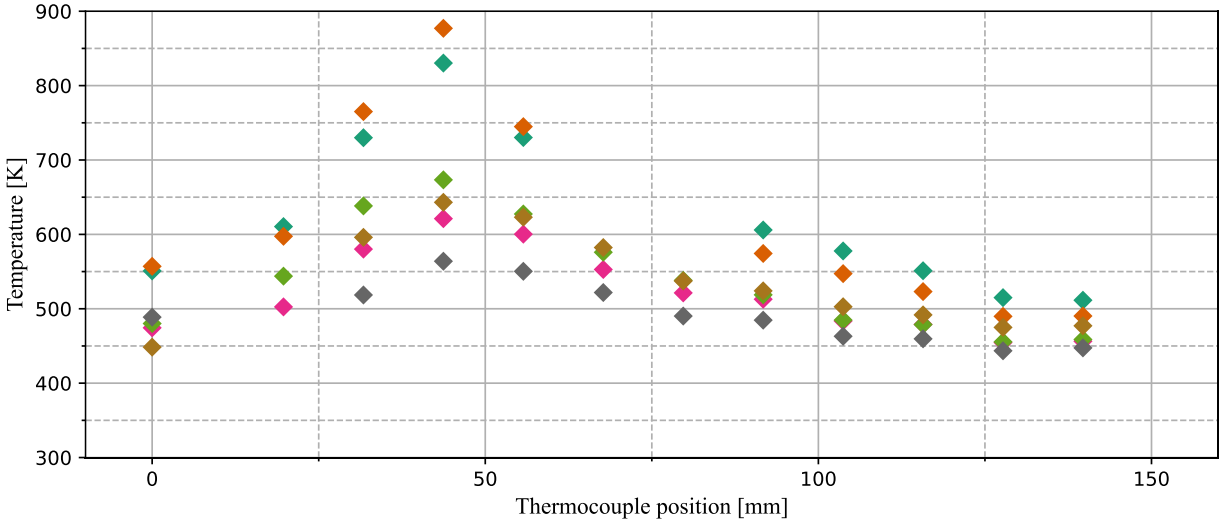

Figure 7: Spatial temperature distribution along the combustion chamber axis averaged between 3,8 and 4 s

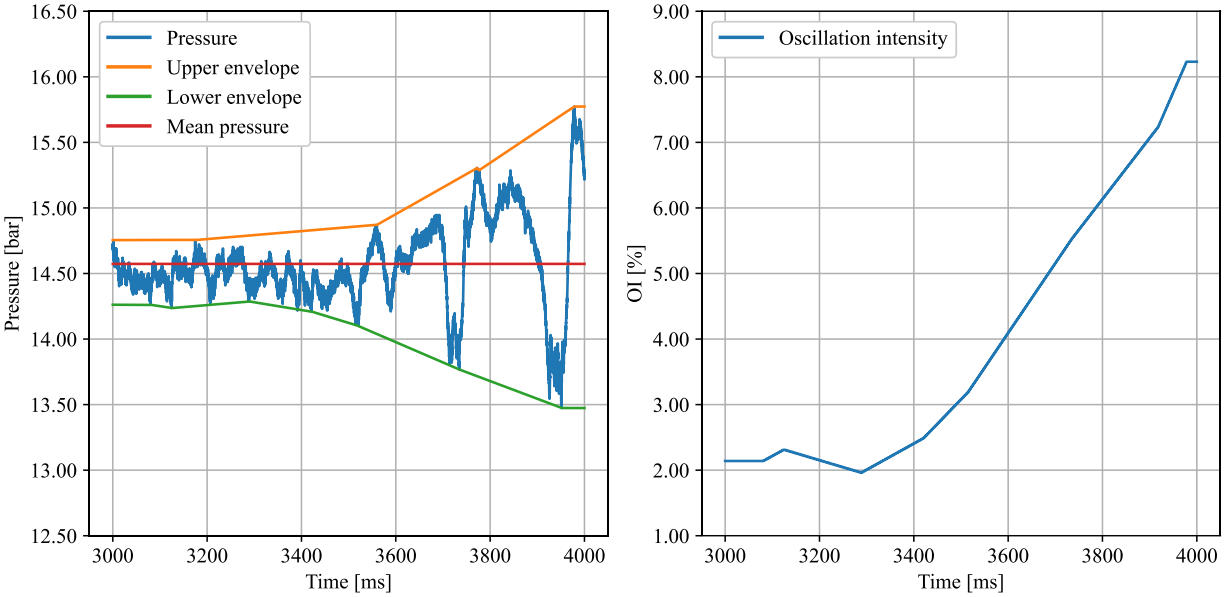

Figure 8: Combustion oscillation intensity calculation in test 313_15

Since the tests were conducted in a heatsink chamber, the wall heating rate should always be positive in this particular area. This positive heating rate can serve as an indicator for long-duration combustion stability. If the chamber wall is observed to be cooling down instead of heating up, it suggests that the combustion is likely to be

extinguished at some point in the future, even if it occurs after the regular experimental combustion time. In the lateral half of the chamber, the heating rate should also be positive, but it may be influenced by heat conduction from the first half. Hence, only the readings from sensors 1 to 5 are taken into account. The heating rate is calculated within the w_1 window using equation 3. If the calculated heating rate falls below zero, one point is deducted from the score.

$$HR = \frac{\bar{T}_{1-5}\left(w_{1,end,};\ w_{1,end,} - 200\ ms\right) - \bar{T}_{1-5}\left(w_{1,start};\ w_{1,start} + 200\ ms\right)}{w_{1,end} - w_{1,start}} \quad \textbf{(3)}$$

$\bar{T}_{1-5}$: mean temperature of sensors 1 – 5 inside a given interval

The third criterion used involves analysing oscillations that occur during combustion. According to [29], rocket combustion is considered stable if the oscillations, referred to as "oscillation intensity" (OI) in this paper, do not exceed ±5% of the average combustion chamber pressure at static operation. To evaluate this metric, the upper and lower envelopes of the pressure signal within the window w_1 are calculated. At least four points are used for each envelope. These points may not always be located at the beginning or end of the signal, so the envelopes are extended along the first and last y-coordinates of the points. Figure 8 depicts the combustion chamber pressure signal along with the corresponding envelopes for test 313_15 as an example.

The oscillation intensity is determined across the entire interval of w_1 (3000 to 4000 ms as shown in Figure 8). However, for evaluation purposes, only the mean value within the w_2 window (3750 to 4000 ms in this case) is considered. This approach allows us to capture any changing dynamics or instabilities that may arise towards the end of the experiment, as observed in the case of test 313_15. In test 313_15, the oscillation intensity value within this interval is calculated to be 5.67%, indicating a decrease in stability score by one point. The oscillation intensity value is calculated using the following equation:

$$OI = \frac{max\left\{\left|env_{hi,t} - \overline{P_{w1}}\right|; \left|env_{lo,t} - \overline{P_{w1}}\right|\right\}}{\overline{P_{w1}}}, \qquad \forall\ t\ \in w_1 \quad \textbf{(4)}$$

$env_{hi,t}$: upper envelope value at *t*;
$env_{lo,i}$: lower envelope value at *t*;
$\overline{P_{w1}}$: mean pressure inside w_1

To account for longer-term tendencies in the combustion chamber pressure another criterion is used. Analogously to the oscillation intensity criterion a rating deprecation by one takes place if the mean pressure drops more than 5% inside the w1 window. The formula for calculating the pressure rate (i.e. pressure change over time) is similar to the one used for the heating rate and is given by the following equation:

$$PR\ = \frac{\bar{P}\left(w_{1,end,};\ w_{1,end,} - 50\ ms\right) - \bar{P}\left(w_{1,start};\ w_{1,start} + 50\ ms\right)}{\overline{P_{w1}}} \quad \textbf{(5)}$$

4. Results and discussion

Figure 8 presents the final results of the test series 31X and 6XX. It's important to note that while the combustion efficiency η_{C*} is affected by measurement uncertainties, primarily due to throat diameter variations, the figure does not include error bars intentionally. This decision was made to avoid cluttering the image with excessive details.

As mentioned earlier, the test campaign followed a stepwise approach to gradually reduce tank pressure and, consequently, propellant mass flow into the chamber until stable combustion was no longer possible. To cover a wider pressure range, some tank pressure load points only have one valid test case available. However, for the low-pressure operation limit, at least three tests were conducted both above and below the limit. Using the ignition procedure implemented in test series 6XX, the low-pressure operation limit for NMP-001 was determined to be between 14.5 and 15 bar. The six experiments that defined this limit were conducted in rapid succession with

minimal nozzle erosion between them. The characteristic length L* for these six experiments was 11.6 m. In all other tests, L* varied between 9.0 and 11.6 m due to nozzle throat erosion.

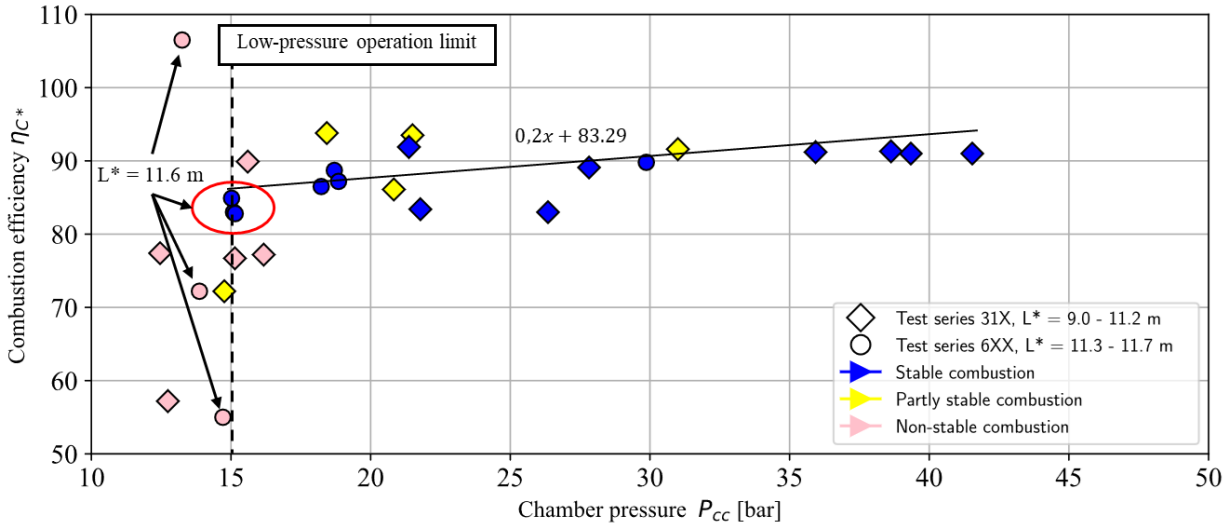

Figure 8: NMP-001 combustion efficiency at varying operation pressures

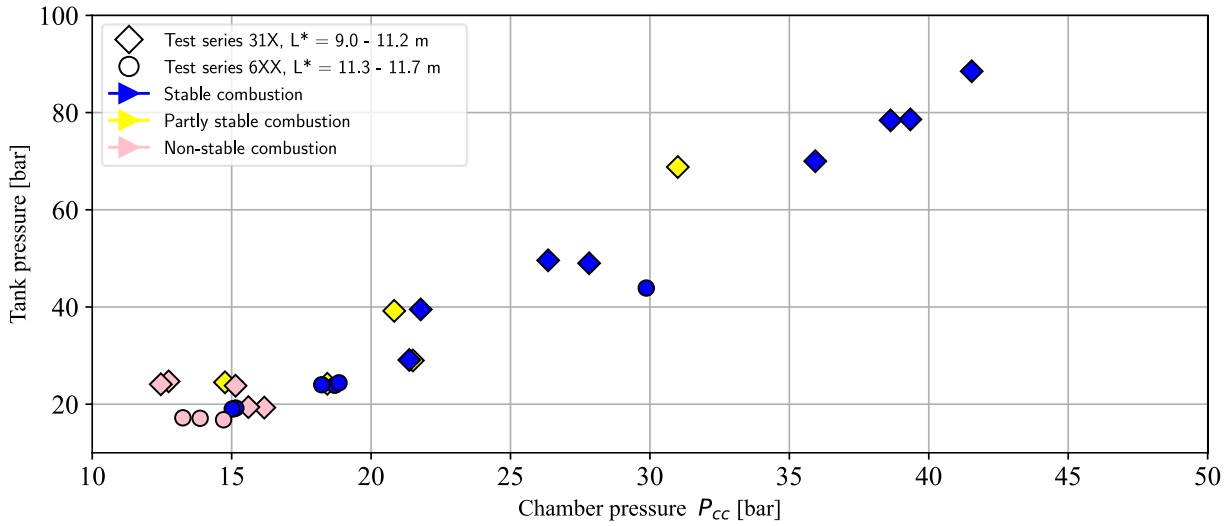

Figure 9: Load points used in tests series 31X and 6XX

However, it is evident from Figure 6 in the case of test 618_1, that it cannot be conclusively determined that NMP-001 would operate only at the mentioned low pressures. This uncertainty arises because the injector was not optimized for operation with such low mass flows. Consequently, it failed to provide an adequate pressure drop, which could potentially have led to a flameout shortly after the igniter was switched off due to insufficient or reduced propellant mass flow during the ignition phase, similar to what was observed in test series 31X. Nevertheless, Figure 9 demonstrates that even with a non-optimized fluid system and injector, the operation at tank pressures commonly used in spacecraft and satellite propulsion, i.e. inside the 20 – 30 bar tank pressure range, is achievable. The combustion efficiency at lower combustion chamber pressures is slightly lower compared to higher pressures. Approximately 0.2% efficiency increase per 1 bar of chamber pressure increase can be observed as shown by the linear trendline in figure 8. This may be attributed to the pressure-dependent nature of nitromethane's decomposition mechanism. However, the highest achieved combustion efficiency in a stable test reached 93.6% at 18 bar. Conversely, the lowest recorded efficiency was 82.8% in test 620_2. Notably, these values could be further improved by employing a non-battleship combustion chamber design, which would have a shorter characteristic length L* and consequently a reduced heat-sink effect.

In comparison to the combustion experiment data described in [21] for nitromethane-based propellants with transition metal catalysts, the combustion of NMP-001 exhibited considerably greater stability at lower pressures. Notably, a low-pressure operation limit of 15 bar could be successfully demonstrated for NMP-001, which represents a significant improvement over the previously reported limit of 30 bar in [21].

5. Conclusion and Outlook

In this paper, the combustion behavior of NMP-001, a nitromethane-based monopropellant with tailored additives to enhance its low-pressure combustion performance and sensitivity to mechanical stimuli, was investigated. The tests conducted revealed a significant reduction in the low-pressure operation limit compared to the literature for other nitromethane-based propellants. At a characteristic length L* of 11.6 m, stable combustion was achieved at 15 bar, which is significantly below the 30 bar limit reported in [21] for a similar characteristic chamber length. However, due to the non-optimized injector and the complex influence of the H_2/O_2 torch ignitor used for propellant initiation, it remains uncertain whether even lower combustion chamber pressures can be reached. Nonetheless, the study demonstrates that NMP-001 is capable of producing thrust at combustion chamber pressures and tank pressure levels commonly employed in satellite and spacecraft propulsion systems.

The combustion efficiency ranging from 82.6% to 93.6% is not yet considered satisfactory. This discrepancy may be attributed to the utilization of a relatively large heat-sink chamber. Therefore, future research should focus on characterizing the combustion in chambers with smaller L* values. Additionally, although the H_2/O_2 torch ignitor proved reliable for ignition, its usage complicated the accurate characterization of the combustion behavior. Moreover, from a system engineering perspective, employing a bulky and cumbersome H_2/O_2 system for ignition in satellite or spacecraft propulsion systems is undesirable. Thus, there is a need to develop alternative ignition methods better suited for the intended application of this propellant.

References

[1] ECHA (European Chemicals Agency), 2006. Agreement of the Member State Committee on the Identification of Hydrazine as a Substance of Very High Concern.

[2] Masse, R., Allen, M., Spores, R., and Driscoll, E. A., 2016. AF-M315E propulsion system advances and improvements. In: *52nd AIAA/SAE/ASEE Joint Propulsion Conference*. 4577.

[3] Bombelli, V., Simon, D., Moerel, J. L., & Marée, T., 2003. Economic benefits of the use of non-toxic mono-propellants for spacecraft applications. In: 39th *AIAA/ASME/SAE/ASEE Joint Propulsion Conference and Exhibit*. 4783.

[4] Haynes, W. M., 2016. CRC handbook of chemistry and physics. 2016

[5] Wingborg, N., Eldsäter, C., and Skifs, H., 2004. Formulation and characterization of ADN-based liquid monopropellants. *In: ESA Special Publication.* Vol. 557.

[6] Persson, M., Anflo, K., and Friedhoff, P., 2019. Flight heritage of ammonium dinitramide (ADN) based high performance green propulsion (HPGP) systems. *Propellants, Explosives, Pyrotechnics.* 44:9, 1073-1079.

[7] Dinardi, A., Anflo, K., and Friedhoff, P., 2017. On-orbit commissioning of high-performance green propulsion (HPGP) in the SkySat constellation. In: *31st AIAA/USU Conference on Small Satellites*.

[8] Katsumi, T., & Hori, K., 2021. Successful development of HAN based green propellant. *Energetic Materials Frontiers*, 2(3), 228-237.

[9] Masse, R. K., Spores, R., & Allen, M., 2020. AF-M315E advanced green propulsion–GPIM and beyond. In: *AIAA Propulsion and Energy 2020 Forum*. 3517.

[10] Colón, B. J., Glaser, M. J., Lightsey, E. G., Bruno, A. R., Cavender, D. P., and Lozano, P., 2022, Spectre: Design of a Dual–Mode Green Monopropellant Propulsion System. *AAS-094*.

[11] Hori, K., Katsumi, T., Sawai, S., Azuma, N., Hatai, K., and Nakatsuka, J., 2019. HAN-Based Green Propellant, SHP163–Its R&D and Test in Space. *Propellants, Explosives, Pyrotechnics*. 44:9, 1080-1083.

[12] Boyer, E., and Kuo, K., 2006. Characteristics of nitromethane for propulsion applications, *In: 44th AIAA Aerospace Sciences Meeting and Exhibit*. 361.

[13] House, W. C., 1947. Project SQUID. Liquid Propellant Rockets. Volume 2, Part 2. *Princeton Univ. NJ*

[14] Clark, J. D., 1972. Ignition!: An informal history of liquid rocket propellants. *New Brunswik: Rutgers University Press,* 1972.

[15] Makovky, A., and Lenji, L, 1958. Nitromethane-physical properties, thermodynamics, kinetics of decomposition, and utilization as fuel, *Chemical Reviews*,58:4, 627-644.

[16] Hermoni, A.,1959. Role of rate of decomposition of nitric oxide in the use of nitromethane as a monopropellant. *J. Appl. Chem*. 9:8, 420-422.
[17] Benziger, J. B., 1982. Decomposition of Nitromethane over NiO and Cr_2O_3 Catalysts. *Combustion Science and Technology*, 29:3-6, 191-205.
[18] Benziger, J. B., 1984. A mechanistic study of nitromethane decomposition on nickel. *Applications of surface science*, 17:3, 309-323.
[19] Gordon, S., & McBride, B. J., 1994. Computer program for calculation of complex chemical equilibrium compositions and applications. Part 1: Analysis. *No. NAS 1.61: 1311*.
[20] Bellinger, F., Friedman, H. B., Bauer, W. H., Eastes, J. W., and Bull, W. C., 1948. Chemical Propellants. Mononitromethane. *Industrial & Engineering Chemistry*, 40:7, 1324-1331.
[21] Kindsvater, H. M., Kendall, K. K., Mueller, K. H., and Datner, P. P., 1951. Research on nitromethane. *Aerojet Engineering Corp. Azusa, CA*.
[22] Shrestha, K. P., Vin, N., Herbinet, O., Seidel, L., Battin-Leclerc, F., Zeuch, T., and Mauss, F., 2020. Insights into nitromethane combustion from detailed kinetic modeling–Pyrolysis experiments in jet-stirred and flow reactors. *Fuel*, 261, 116349.
[23] Hermoni, A., and Gruenwald, T. B., 1964. The Thermal Decomposition of Nitroethane Under High Pressure. *Nitro Compounds*. 225-233
[24] Kurilov, M., Ziemer, L., Weiser, V., Ricker S., Kirchberger C., U., Schlechtriem S., 2023. Ignition of Nitromethane-based Propellant Mixtures. In: *13ISICP*, in publication.
[25] Bellinger, F., Friedman, H. B., Bauer, W. H., Eastes, J. W., and Bull, W. C., 1948. Chemical Propellants. Stability of Mononitromethane. *Industrial & Engineering Chemistry*, 40:7 1320-1323.
[26] Campbell, A. W., Malin, M. E., and Holland, T. E., 1956. Temperature effects in the liquid explosive, nitromethane, *J. of Appl. Phys*., 27:8, 963-963.
[27] Kurilov, M., Werling, L., Negri, M., Kirchberger, C., & Schlechtriem, S., 2023. Impact Sensitivity of Nitromethane-based Green-propellant Precursor Mixtures. *International Journal of Energetic Materials and Chemical Propulsion*, 22:2, 35-43.
[28] Kurilov, M., Kirchberger, C., Freudenmann, D., Stiefel, A. D., and Ciezki, H., 2018. A method for screening and identification of green hypergolic bipropellants, *International Journal of Energetic Materials and Chemical Propulsion*, 17:3, 183-203.
[29] Sutton, G. P., and Biblarz, O., 2016. Rocket propulsion elements. *John Wiley & Sons*.
[30] Brown, C. D., 1996. Spacecraft propulsion. *AIAA*.
[31] Suslov, D., Woschnak, A., Sender, J., Oschwald, M., and Haidn, O., 2003. Test specimen design and measurement technique for investigation of heat transfer processes in cooling channels of rocket engines under real thermal conditions. In: *39th AIAA/ASME/SAE/ASEE Joint Propulsion Conference and Exhibit*, 4613.
[32] Kayser, J. C., and Shambaugh, R. L., 1991. Discharge coefficients for compressible flow through small-diameter orifices and convergent nozzles. *Chemical engineering science*, 46:7, 1697-1711.